PNAS RESEARCH ARTICLE | MEDICAL SCIENCES

Inhibition of CDK8/19 Mediator kinase potentiates HER2-targeting drugs and bypasses resistance to these agents in vitro and in vivo

Xiaokai Ding[a], Amanda C. Sharko[a], Martina S. J. McDermott[a], Gary P. Schools[a], Alexander Chumanevich[a], Hao Ji[a], Jing Li[a], Li Zhang[a], Zachary T. Mack[a], Vitali Sikirzhytski[a], Michael Shtutman[a], Laura Ivers[b], Norma O'Donovan[b], John Crown[b], Balázs Győrffy[c,d], Mengqian Chen[a,e], Igor B. Roninson[a], and Eugenia V. Broude[a,1]

Edited by Myles Brown, Dana-Farber Cancer Institute, Boston, MA; received January 23, 2022; accepted June 28, 2022

Breast cancers (BrCas) that overexpress oncogenic tyrosine kinase receptor HER2 are treated with HER2-targeting antibodies (such as trastuzumab) or small-molecule kinase inhibitors (such as lapatinib). However, most patients with metastatic HER2$^+$ BrCa have intrinsic resistance and nearly all eventually become resistant to HER2-targeting therapy. Resistance to HER2-targeting drugs frequently involves transcriptional reprogramming associated with constitutive activation of different signaling pathways. We have investigated the role of CDK8/19 Mediator kinase, a regulator of transcriptional reprogramming, in the response of HER2$^+$ BrCa to HER2-targeting drugs. CDK8 was in the top 1% of all genes ranked by correlation with shorter relapse-free survival among treated HER2$^+$ BrCa patients. Selective CDK8/19 inhibitors (senexin B and SNX631) showed synergistic interactions with lapatinib and trastuzumab in a panel of HER2$^+$ BrCa cell lines, overcoming and preventing resistance to HER2-targeting drugs. The synergistic effects were mediated in part through the PI3K/AKT/mTOR pathway and reduced by PI3K inhibition. Combination of HER2- and CDK8/19-targeting agents inhibited STAT1 and STAT3 phosphorylation at S727 and up-regulated tumor suppressor BTG2. The growth of xenograft tumors formed by lapatinib-sensitive or -resistant HER2$^+$ breast cancer cells was partially inhibited by SNX631 alone and strongly suppressed by the combination of SNX631 and lapatinib, overcoming lapatinib resistance. These effects were associated with decreased tumor cell proliferation and altered recruitment of stromal components to the xenograft tumors. These results suggest potential clinical benefit of combining HER2- and CDK8/19-targeting drugs in the treatment of metastatic HER2$^+$ BrCa.

CDK8/19 | Mediator kinase | HER2 | lapatinib | trastuzumab

Significance

Breast cancers that overexpress oncogenic tyrosine kinase receptor HER2 are treated with HER2-targeting antibodies (such as trastuzumab) or small-molecule kinase inhibitors (such as lapatinib). However, most patients with metastatic HER2$^+$ breast cancer have intrinsic resistance and nearly all eventually become resistant to HER2-targeting therapy. Resistance to HER2-targeting drugs frequently involves transcriptional reprogramming associated with constitutive activation of different signaling pathways. We have found that inhibition of CDK8/19 Mediator kinase, a regulator of transcriptional reprogramming, sensitizes HER2$^+$ breast cancers to HER2-targeting drugs, overcoming and preventing drug resistance, both in vitro and in vivo. These results suggest that combining HER2 and CDK8/19-targeting drugs could greatly improve the treatment outcome in metastatic HER2$^+$ breast cancer.

Approximately 20% of breast cancers (BrCas) overexpress oncogenic tyrosine kinase receptor HER2/NEU, a member of the epidermal growth factor receptor (EGFR) family. HER2$^+$ patients are treated with HER2-targeting drugs, including monoclonal antibodies trastuzumab and pertuzumab, small-molecule HER2/EGFR kinase inhibitors lapatinib and neratinib, and T-DM1, a conjugate of trastuzumab with a cytotoxic drug (emtansine) (1). Despite the transformative effect of HER2-targeting drugs in the adjuvant setting, nearly 70% of metastatic HER2$^+$ BrCas have intrinsic resistance and nearly all become resistant to HER2-targeting therapy after an initial response. Many of the varied mechanisms of resistance to HER2-targeting drugs involve transcriptional reprogramming associated with constitutive activation of signaling pathways parallel or downstream of HER2 (2). Overcoming or preventing resistance to HER2-targeting drugs could transform the management of patients with metastatic HER2$^+$ BrCa.

CDK8 (ubiquitously expressed) and CDK19 (expressed in some cell types) are two isoforms of Mediator kinase, the enzymatic component of the CDK module that binds to the transcriptional Mediator complex. In addition to CDK8 or CDK19, the CDK module includes Cyclin C, MED12, and MED13 (3). Unlike better-known CDKs (such as CDK4/6), CDK8/19 regulate transcription but not cell cycle progression. In contrast to other transcriptional CDKs, such as CDK7 or CDK9, Mediator kinase is not a part of the overall transcription machinery (3) but acts as a cofactor or modifier of several cancer-relevant transcription factors, including β-catenin/TCF/LEF (4), SMADs (5, 6), Notch (7), STATs (8), HIF1α (9), ER (10), NFκB (11), and MYC (12). CDK8/19 Mediator kinase directly phosphorylates some transcription factors (SMADs, STATs, and Notch) and in other cases acts through C-terminal phosphorylation of RNA polymerase II (Pol II), enabling the elongation of transcription. Importantly, CDK8/19 affect Pol II phosphorylation not globally but only in the context of

Competing interest statement: M.C. is an employee and I.B.R. is president of Senex Biotechnology, Inc., and E.V.B. and J.L. are consultants for Senex Biotechnology, Inc.

This article is a PNAS Direct Submission.

[1]To whom correspondence may be addressed. Email: broude@cop.sc.edu.

This article contains supporting information online at http://www.pnas.org/lookup/suppl/doi:10.1073/pnas.2201073119/-/DCSupplemental.

Published August 1, 2022.

newly induced genes, impacting primarily de novo–induced but not basal transcription (11). With this unique activity, CDK8/19 have been identified as regulators of transcriptional reprogramming (11, 13, 14). CDK8 is required for embryonic development, which is driven by transcriptional reprogramming (15, 16), but conditional CDK8 knockout in adult animals yields no phenotype (17). Although systemic toxicity was reported for two CDK8/19 inhibitors (CDK8/19i) (18), this toxicity was later found to be due to off-target effects (19), and two other CDK8/19i have entered clinical trials (clinicaltrials.gov NCT03065010 and NCT04021368).

CDK8 protein is elevated in the invasive ductal carcinoma of the breast (20) and correlated with tumor stage, nodal status, and shorter relapse-free survival (RFS) (21). CDK8 expression in BrCa shows strong positive correlation with p53 mutant status and MYC expression (20) and negative correlations with the expression of ERα (10). RNA expression of CDK8 and its interactive proteins correlates with shorter RFS in BrCa (20, 22); such correlations are much stronger in patients receiving systemic therapy than in untreated patients, indicating that Mediator kinase is associated with therapy failure (20). Selective CDK8/19i inhibit estrogen-induced transcription and mitogenic stimulation in ER^+ BrCa cells, inhibit the growth of ER^+ BrCa xenografts, and potentiate the effect of the antiestrogen fulvestrant (10).

In the present study, we have analyzed the effects of CDK8/19 inhibition, using two chemically distinct selective CDK8/19i, on the response of $HER2^+$ BrCa cell lines to HER2-targeting small molecules and trastuzumab in vitro and investigated in vivo effects of a potent CDK8/19i alone and in combination with lapatinib in xenografts formed by lapatinib-sensitive or -resistant $HER2^+$ BrCa cells. Our results show that CDK8/19 inhibition has a synergistic effect with HER2-targeting agents and overcomes resistance to HER2-targeting drugs, in vitro and in vivo. The synergy is mediated in part through the PI3K/AKT/mTOR pathway and associated with cooperative inhibition of STAT1 and STAT3 phosphorylation at S727 by CDK8/19- and HER2-targeting agents. These results suggest potential utility of combining HER2- and CDK8/19-targeting drugs in the treatment of metastatic $HER2^+$ BrCa.

Results

Expression of CDK8 and Its Interactive Genes Is Associated with Faster Relapse in Treated $HER2^+$ BrCa Patients. We have used the Kaplan–Meier plotter (23) to investigate correlations between CDK8 RNA expression (based on microarray data with long-term followup) and RFS in $HER2^+$ BrCa patients, stratified into groups that did or did not receive treatment after sample collection. Treated patients showed much shorter RFS if their tumors belonged to the upper tertile for the expression of CDK8 (hazard ratio [HR] = 1.87, $P = 3.4e-05$), but there was no correlation with RFS among untreated patients (*SI Appendix*, Fig. S1). To compare the predictive power of CDK8 relative to other genes, the same analysis was repeated for all the genes in $HER2^+$ BrCa-treated patients and the genes were ranked based on their achieved HR values. CDK8 ranked in the top 1% (#77 of 10,091) of genes by the correlation of its higher expression with shorter RFS. We then used Pharos analysis (24) to identify "druggable" genes, categorized as Tchem (small molecules are known to modulate the protein) or Tclin (approved drugs exist for this target). RFS correlations for the top 50 druggable genes are shown in *SI Appendix*, Table S1. CDK8 ranked #15 of 1,377 Tchem targets and above all but one of 498 Tclin targets. We have also tested RFS correlations for CDK19 (the paralog of CDK8) and CDK8/19-interactive proteins CCNC, MED12, and MED13. CCNC and MED13 showed strong RFS correlations in treated $HER2^+$ BrCa patients (ranking in the top 5% of all genes), with a weaker correlation for CDK19 but no significant correlation for MED12 in concordance with previous findings for this gene in other BrCa subtypes (20). As with CDK8, no significant survival correlations for other CDK module subunits were observed among untreated patients (*SI Appendix*, Fig. S1). These observations suggest that CDK8 with its interactive genes may play a unique role as a determinant of treatment response in $HER2^+$ BrCa patients.

Effects of CDK8/19 Inhibition on Cellular Response to HER2-Targeting Drugs. We have tested the interactions between two anti-HER2 drugs, the small-molecule kinase inhibitor lapatinib and the monoclonal antibody trastuzumab, and two chemically distinct selective CDK8/19i, senexin B (10) and SNX631 (also known as 15u) (25). *SI Appendix*, Table S2 provides the chemical formulas and compares the activities of senexin B and SNX631 in a battery of cell-free and cell-based assays for CDK8/19 inhibition (26). SNX631 was 6 to 10 times more potent than senexin B in all the assays except for the DiscoverX active-site–dependent competition binding assay. The latter assay uses recombinant CDK8 and CDK19 proteins without their cyclin partner CCNC; as previously discussed, the absence of CCNC has differential effects on the binding affinities of different CDK8/19i (19). Five $HER2^+$ BrCa cell lines were treated for 7 d with HER2 and CDK8/19i individually and in fixed-ratio combinations (Fig. 1 *A*–*E*). These cell lines included parental HCC1954 (HCC1954-Par) cells (Fig. 1*A*) and their derivative HCC1954-Res selected for acquired resistance to lapatinib (27) (Fig. 1*B*), JIMT-1 (Fig. 1*C*), SKBR3 (Fig. 1*D*), and BT474, the only cell line in this panel that is both $HER2^+$ and ER^+ (Fig. 1*E*). Synergy was determined on the basis of combination index (CI) values calculated using CompuSyn (28). SKBR3, BT474, and, to a lesser extent, HCC1954-Par are inherently sensitive to lapatinib, the other cell lines being relatively resistant. Trastuzumab had little effect on in vitro growth of most of these cell lines, except for BT474. CDK8/19i alone had only minor or no effects on the growth of most cell lines except for BT474; the effect of CDK8/19 inhibition in such ER^+ cells is mediated through the effect of CDK8 on the transcriptional activity of ER (10). Combining HER2 and CDK8/19i increased the growth-inhibitory effect in every case (Fig. 1 *A*–*E*). Moreover, these effects were synergistic in all cases (as indicated by CI values less than 1.0), except for the additive effect of trastuzumab + senexin B combination in SKBR3 cells. Remarkably, synergy was observed not only in lapatinib-sensitive cell lines but also in cells with inherent or acquired resistance to HER2-targeting drugs. Lapatinib-selected HCC1954-Res cells showed cross-resistance to the small-molecule HER2 inhibitor neratinib relative to HCC1954-Par, but the addition of senexin B potentiated the effects of neratinib on both cell lines, reversing the acquired resistance (*SI Appendix*, Fig. S2).

We have also tested the effects of CDK8/19i on the development of adaptive lapatinib resistance in a previously described short-term single-step adaptation procedure (29). Both SKBR3 (Fig. 1*F*) and BT474 cells (Fig. 1*G*) were growth-inhibited by 250 nM lapatinib after 1 wk of treatment, but cell colonies growing in the presence of the drug became apparent after 4 to 8 wk. After 16 wk, extensive cell growth was observed despite the presence of lapatinib (Fig. 1 *F* and *G*), indicating drug adaptation. While senexin B alone had only a

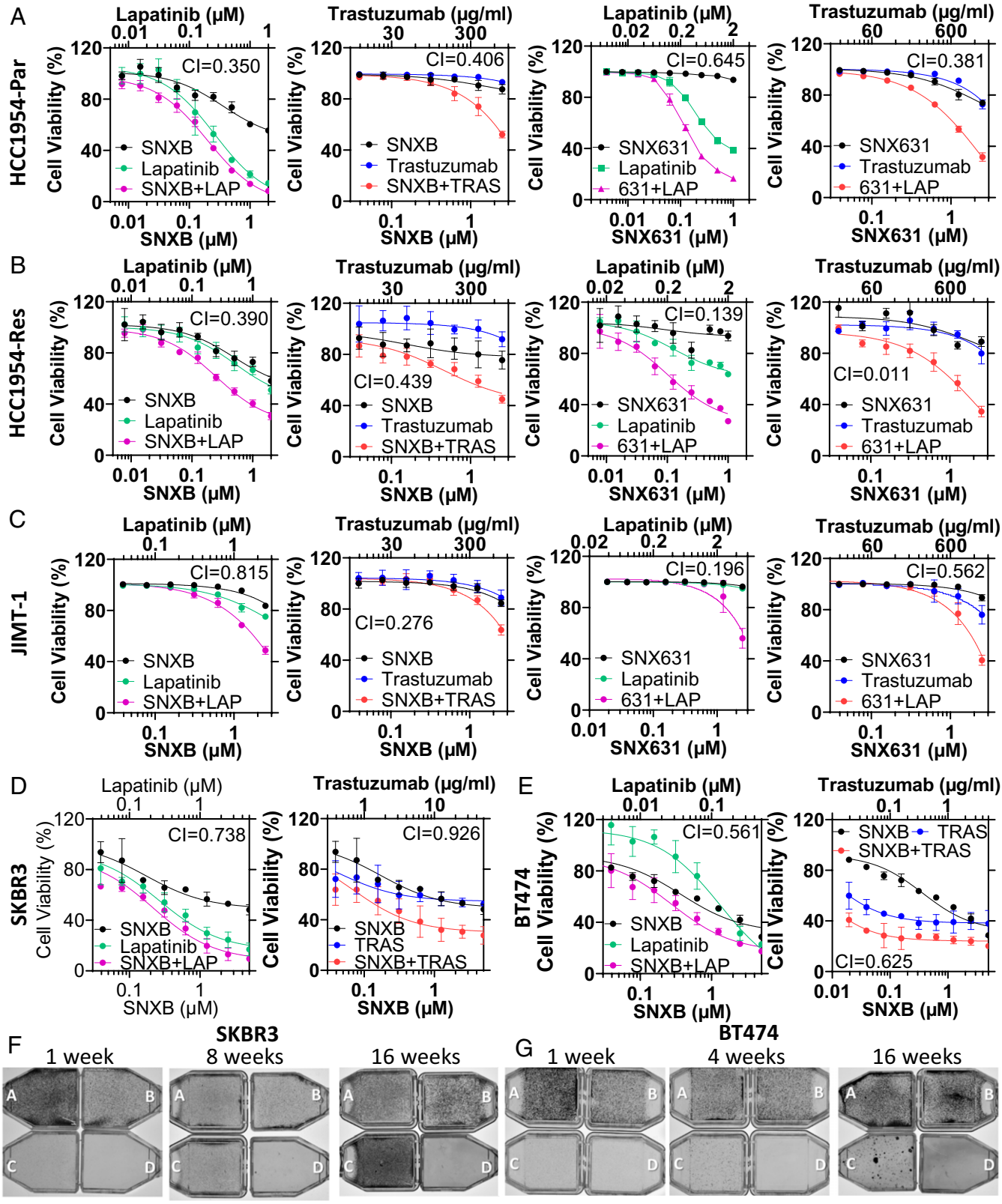

Fig. 1. Effects of CDK8/19 inhibition on the responses to lapatinib and trastuzumab in HER2$^+$ BrCA cells. (*A–E*) Seven-day dose–response curves for HER2$^+$ cell lines HCC1954-Par (*A*), HCC1954-Res (*B*), JIMT-1 (*C*), SKBR3 (*D*), and BT474 (*E*), treated with increasing concentrations of lapatinib or trastuzumab, alone or in combination with CDK8/19i senexin B (SNXB) or SNX631. Cell viability data expressed as percent SRB measurements relative to untreated cells ± SD. Combination indices (CIs) are shown in *Upper Right* corner. (*F and G*) Crystal violet staining of flasks with HER2 drug-sensitive cell lines SKBR3 (*F*) and BT474 (*G*) treated continuously with senexin B (2.5 μM; *B*), lapatinib (250 nM; *C*), or their combination (*D*) for 1, 4, 8, and 16 wk (*A*, control).

moderate growth-inhibitory effect, the addition of senexin B to lapatinib almost completely abrogated cell growth even after 16 wk (Fig. 1 *F* and *G*). Hence, combining CDK8/19i with HER2-targeting drugs has a synergistic or additive effect and both overcomes and prevents the development of resistance to the latter agents.

Transcriptomic Analysis of the Effects of Senexin B and Lapatinib in HCC1954 Cells. We have carried out RNA-Sequencing (RNA-Seq) analysis of HCC1954-Par cells treated with dimethyl sulfoxide (DMSO) (control), senexin B alone, lapatinib alone, or lapatinib + senexin B combination for 24 h. We have identified differentially expressed genes (DEGs) by the following criteria: expressed at Fragments Per Kilobase of transcript per Million (FPKM) >1 in at least one condition; fold change (FC) >1.5 between two conditions; and false discovery rate (FDR) <0.05. Lapatinib increased the expression of 224 and decreased the expression of 195 DEGs relative to the control, whereas senexin B up-regulated 61 and down-regulated 32 genes relative to the control and up-regulated 67 and down-regulated 40 DEGs relative to lapatinib. The effects of senexin B on all 419 lapatinib-regulated DEGs are shown in *SI Appendix*, Fig. S3*A*. Senexin B reversed lapatinib-induced changes in 12 DEGs (5 down-regulated and 7 up-regulated) and enhanced lapatinib-induced up-regulation of 7 other DEGs (*SI Appendix*, Fig. S3*B*). Interestingly, 2 of 12 DEGs that showed reversal of lapatinib-induced changes following the addition of senexin B, ALPP and ETV5, are among 5 genes that were up-regulated in common upon selection for trastuzumab resistance in SKBR3 and BT474 cells (30), suggesting that CDK8/19 inhibition may suppress transcriptional pathways associated with resistance to HER2-targeting drugs.

We have used gene set enrichment analysis (GSEA) (31) to determine which of the 50 hallmark pathways were differentially affected by lapatinib alone and by lapatinib + senexin B combination. GSEA plots for the most prominently affected pathways are shown in Fig. 2. Among these, the PI3K/AKT/mTOR pathway geneset was weakly affected by lapatinib alone but showed a strong negative correlation for the combination-treated samples; the effects on differentially affected genes of this pathway are shown in *SI Appendix*, Fig. S3*C* and Table S3. A different impact was observed with two overlapping genesets that are regulated by interferon γ (IFNγ) and IFNα. These pathways were strongly enriched in lapatinib-treated samples but showed a negative correlation when senexin B was added to lapatinib (Fig. 2); the effects on the combined DEGs of these pathways are shown in *SI Appendix*, Fig. S3*D* and Table S4. Based on GSEA analysis, we undertook functional analysis of the role of the most affected pathways on the synergistic interactions between HER2- and CDK8/19-targeting drugs.

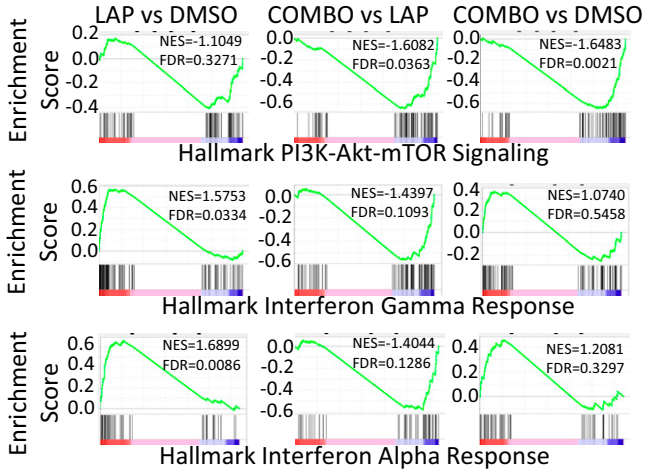

Fig. 2. GSEA analysis of the effects of lapatinib and senexin B on selected genesets. GSEA analyses of the genesets associated with the PI3K/Akt/mTOR (*Top*), INFγ (*Middle*), and INFα (*Bottom*) pathways between treatment groups (lapatinib vs. vehicle, lapatinib + senexin vs. lapatinib, and lapatinib + senexin B vs. vehicle).

PI3K Inhibition Abrogates the Synergistic Effect of CDK8/19 Inhibition on Lapatinib Response. To test the effect of PI3K/AKT/mTOR pathway inhibition on the synergy between HER2 and CDK8/19i, we used two chemically distinct PI3K inhibitors: pictilisib, a pleiotropic inhibitor of different PI3K isoforms, and PI3Kα-specific inhibitor alpelisib. The effect of different PI3K inhibitor (PI3Ki) concentrations on 7-d growth of $HER2^+$ BrCa cell lines HCC1954-Par, HCC1954-Res, and JIMT-1 are shown in Fig. 3*A* (for pictilisib) and Fig. 3*B* (for alpelisib). Pictilisib and (to a lesser extent) alpelisib strongly inhibited the growth of all three cell lines. To analyze the effect of PI3K inhibition on the synergy between HER2 and CDK8/19i, we selected the concentrations of 250 nM pictilisib and 500 nM alpelisib, which inhibited cell growth by ∼25% or less after 7 d (Fig. 3 *A* and *B*) but significantly suppressed PI3K activity as indicated by AKT phosphorylation (Fig. 3 *C* and *D*). We then tested the effects of lapatinib, SNX631, and their fixed-ratio combinations on the same three $HER2^+$ BrCa cell lines in the presence of 250 nM pictilisib or 500 nM alpelisib. Despite their different structures, both PI3Ki had essentially the same effects on the responses of all three cell lines to lapatinib and SNX631 (Fig. 3 *E* and *F*) relative to the effects of these drugs in the absence of PI3Ki (Fig. 1 *A*–*C*). PI3Ki produced a strong sensitization to lapatinib, with no apparent sensitization to SNX631. Furthermore, SNX631 and lapatinib no longer showed synergy in the presence of pictilisib or alpelisib, as indicated by CI values >1 (Fig. 3 *E* and *F*). Notably, the effects of CDK8/19i were not associated with any significant changes in AKT phosphorylation by SNX631 alone or in combination with pictilisib (Fig. 3*C*) or alpelisib (Fig. 3*D*).

Synergistic Effects of HER2 and CDK8/19i on STAT1 and STAT3 S727 Phosphorylation. INFγ and INFα signaling are regulated in part through STAT transcription factors, including STAT1 and STAT3 (32, 33). The activity of these factors is modulated in a complex manner by serine phosphorylation at position 727 (34, 35). CDK8 was shown to be capable of phosphorylating STAT3 (8, 35), a transcription factor implicated in breast carcinogenesis (36), at S727; this phosphorylation was reported to enhance the transcription-stimulating activity of STAT3 (37). STAT1 S727 phosphorylation was also found to be affected by CDK8 (8), in addition to other kinases (19). In contrast to STAT3, STAT1 has been identified as a tumor suppressor in BrCa but S727 phosphorylation of STAT1 may counteract its tumor-suppressive activity (38). We have investigated the effects of lapatinib, trastuzumab, and CDK8/19i on STAT1 and STAT3 phosphorylation at S727, in SKBR3 cells (where senexin B was used as the CDK8/19i) (Fig. 4*A*) and in HCC1954-Par, HCC1954-Res, and JIMT-1 cells (using SNX631 as CDK8/19i) (Fig. 4*B*). CDK8/19i alone decreased STAT1 S727 phosphorylation in all four cell lines. Combining lapatinib and CDK8/19i further decreased this phosphorylation in all the cell lines, whereas lapatinib alone also had noticeable effects in SKBR3 and JIMT-1 cells. Trastuzumab alone did not reduce STAT1 S727 phosphorylation in any cell line tested, but phosphorylation at this site was further reduced by combined trastuzumab–CDK8/19i treatment, as compared to CDK8/19i alone, in three of the tested cell lines. STAT3 S727 phosphorylation was also decreased by CDK8/19i (albeit to a lesser extent than STAT1 phosphorylation). Combined lapatinib–CDK8/19i treatment further decreased phosphorylation at this site in all four cell lines but combining trastuzumab and CDK8/19i augmented the decrease in phosphorylation only in SKBR3 and HCC1954-Res cells. Based on these observations,

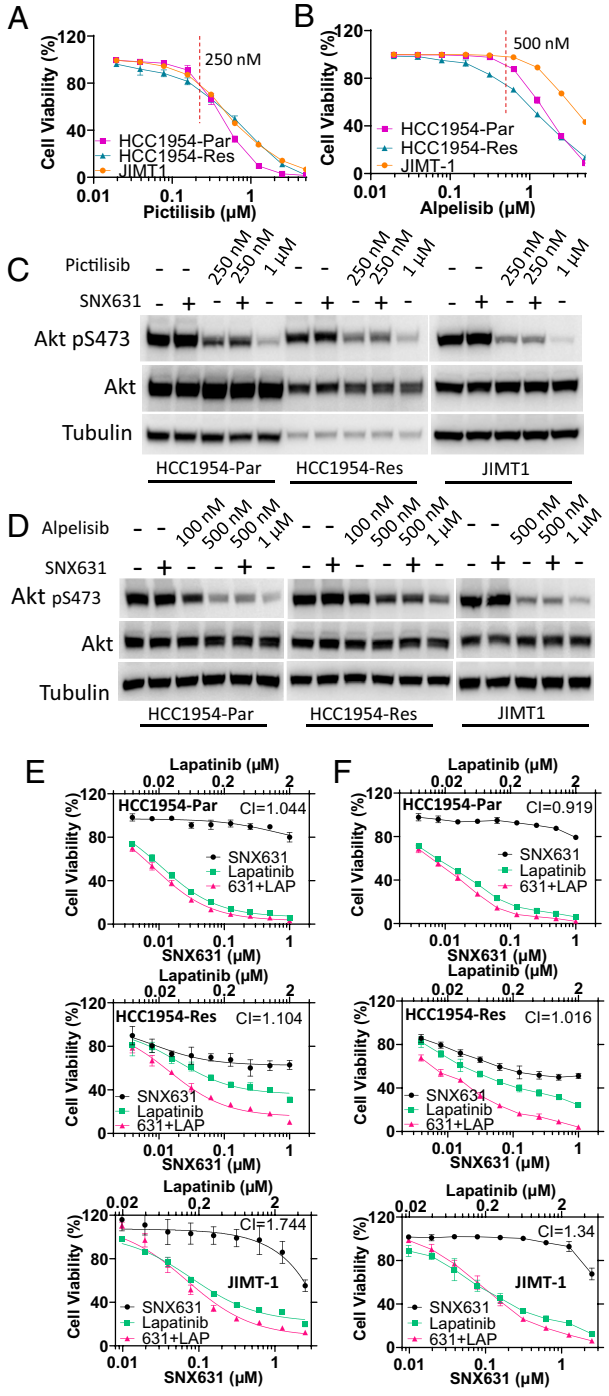

Fig. 3. Effects of PI3K inhibition on the response of HER2$^+$ BrCa cells to lapatinib and SNX631. (*A*) Seven-day dose–response curves for HCC1954-Par, HCC1954-Res, and JIMT-1 cells treated with pan-PI3K inhibitor, pictilisib. Dashed line marks 250 nM pictilisib. (*B*) The same for cells treated with PI3Kα inhibitor alpelisib. (*C*) Western blots showing the effects of 6-h treatment with 250 or 1,000 nM pictilisib and 500 nM SNX631 on phospho-S473 Akt in the same cell lines. (*D*) The same for the effects of 6-h treatment with 100 or 500 nM alpelisib and 500 nM SNX631. (*E*) Seven-day dose–response curves for HCC1954-Par, HCC1954-Res, and JIMT-1 cells treated with 250 nM pictilisib in combination with different concentrations of lapatinib and SNX631. CI values are shown in *Upper Right* corner. (*F*) The same for cells treated with 500 nM alpelisib.

we investigated the role of STAT1 and STAT3 in the resistance to lapatinib and SNX631.

Effects of STAT1 and STAT3 Knockouts in Response to Lapatinib. We carried out CRISPR-Cas9 knockout of STAT1 and STAT3 in HCC1954-Par, HCC1954-Res, and JIMT-1 cells. STAT3 knockout in HCC1954-Par and HCC1954-Res cells led to overexpression of STAT1, as apparent compensatory mechanism, but no reciprocal compensation was observed in these cells after STAT1 knockout (Fig. 4*C*). Such compensation was not seen after STAT1 or STAT3 knockout in JIMT-1 (Fig. 4*C*). We also generated HCC1954-Par and JIMT-1 cells with knockouts of both STAT1 and STAT3 (Fig. 4*C*); however, we were unable to obtain viable HCC1954-Res cells with the knockout of both genes.

We then tested the effects of STAT1 and STAT3 knockouts on lapatinib sensitivity in HCC1954-Par and JIMT-1 cells. The knockout of either STAT1 or STAT3 alone had no effect on lapatinib sensitivity (Fig. 4*D*) but the knockout of both STATs sensitized both cell lines to lapatinib (Fig. 4*E*), indicating a cooperative effect. The knockout of STAT1 + STAT3 slightly sensitized HCC1954-Par but not JIMT-1 to SNX631 alone (Fig. 4*F*), while reducing the synergy between lapatinib and SNX631 in HCC1954-Par (CI = 0.954) seemingly abolished such synergy in JIMT-1 (Fig. 4*G*; CI could not be calculated in JIMT-1 due to minimal effect of SNX631). These results implicate STAT1 and STAT3 as cooperating factors in lapatinib sensitivity and as variable determinants in the synergy between HER2- and CDK8/19-targeting agents.

Effects on MicroRNAs Regulating Drug Response in HER2$^+$ BrCa and on BTG2 Tumor Suppressor. We have previously found that the effects of Mediator kinase on metastatic growth of colon cancer are mediated by a microRNA (miR) (39). Some oncogenic miRs have been implicated in HER2 BrCa drug response, as well as in STAT and PI3K/AKT/mTOR signaling. In particular, miR-21 is up-regulated by and targets STAT3 (40, 41); and decreased miR-21 was correlated with better survival of HER2$^+$ BrCa patients (42). Silencing of miR-21 also confers sensitivity to tamoxifen and fulvestrant in BrCa through inhibition of the PI3K/AKT/mTOR pathway (43). Another microRNA, miR-221, confers lapatinib resistance in HER2$^+$ BrCa (44) and gefitinib resistance in cervical cancer (45) and has been implicated as a regulator of both PI3K/AKT/mTOR (45) and STAT pathways (46, 47). We used qPCR to measure the expression of miR-21 for both its guide strand (miR-21-5p) and passenger strand (miR-21-3p) and of miR-221 (guide strand) expression in parental and resistant HCC1954 cells. The cells were untreated or treated with lapatinib, SNX631, or their combination. As shown in Fig. 5*A*, all three miRs were up-regulated by lapatinib or SNX631 individually in both cell lines, but no up-regulation was observed upon treatment with the drug combination.

A prominent target of miR-21 is the tumor suppressor gene BTG2, which is involved in cell differentiation, proliferation, apoptosis, and other cellular functions (48). qPCR analysis showed that BTG2 was strongly up-regulated in both HCC1954-Par and HCC1954-Res cells by the combination of lapatinib and senexin B, with much weaker effects of individual drugs (Fig. 5*B*). To determine whether BTG2 expression contributes to the response to HER2 and CDK8/19i, we used shRNA transduction to decrease BTG2 expression (Fig. 5*C*). BTG2 knockdown made these cells more resistant to lapatinib, SNX631, and their combination (Fig. 5*D*), suggesting that induction of this tumor suppressor may mediate the antiproliferative effect of HER2 and CDK8/19i.

CDK8/19i Suppresses In Vivo Tumor Growth and Potentiates Lapatinib in Lapatinib-Sensitive and Resistant HER2$^+$ BrCa Xenografts. We have tested the effects of in vivo treatment with lapatinib and SNX631 in HCC1954-Par and HCC1954-Res xenografts in NOD.*Cg-Prkdc^{scid}Il2rg^{tm1Wjl}*/SzJ (NSG) mice.

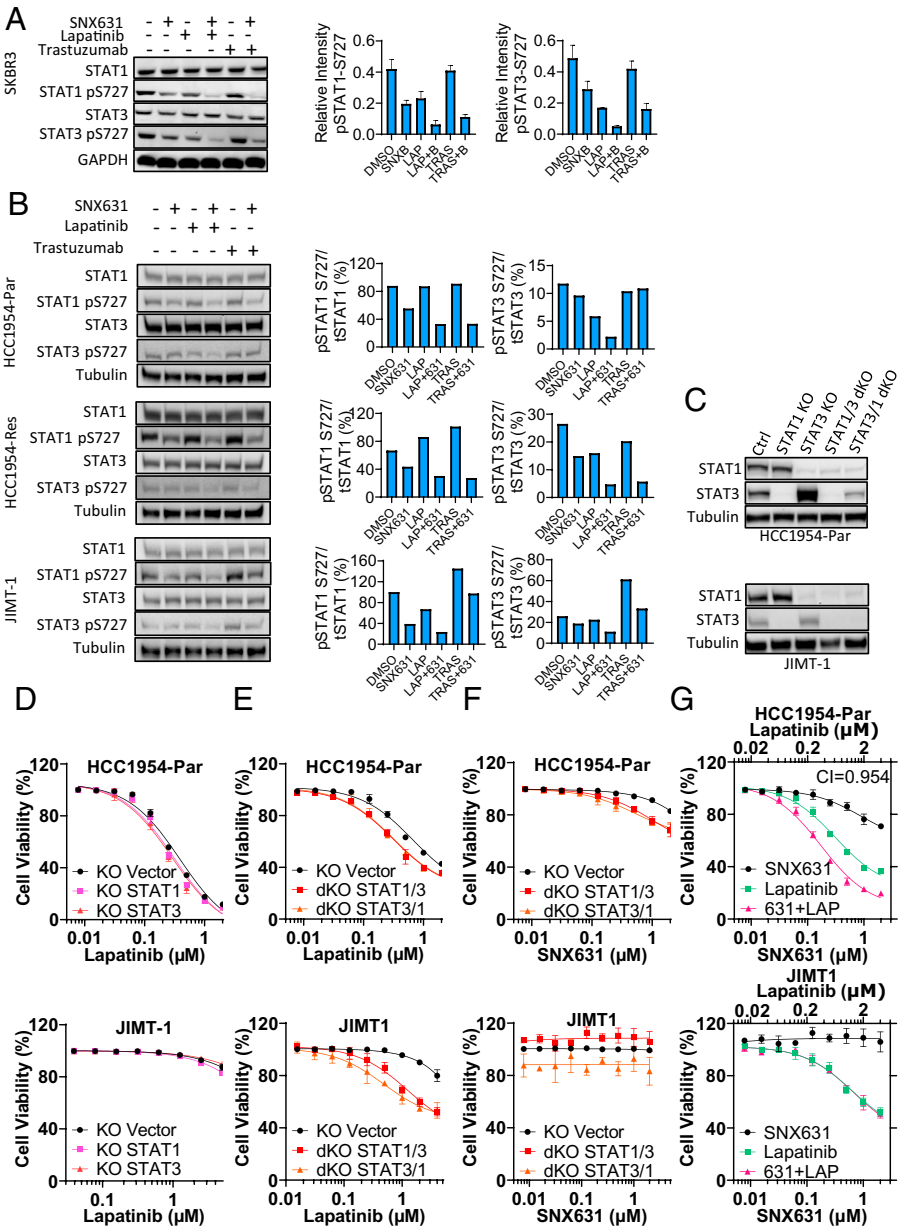

Fig. 4. STAT1 and STAT3 interactions with CDK8/19 and HER2 inhibitors. (*A*) Representative Western blots (with densitometric measurements, mean ± SEM of three independent experiments) showing the effects of lapatinib or trastuzumab, alone or in combination with senexin B on phosphorylation of STAT1 S727 and STAT3 S727 in SKBR3 cells. (*B*) The same for the effects of lapatinib or trastuzumab, alone or in combination with SNX631 on phosphorylation in HCC1954-Par, HCC154-Res, and JIMT-1 cells. (*C*) Representative Western blots showing CRISPR-Cas9 knockout efficiency of STAT1 and STAT3, individually (STAT1 knockout [KO] and STAT3 KO), and in sequential combinations (double KO [dKO] STAT1/3 and dKO STAT3/1) in HCC1954-Par, HCC1954-Res, and JIMT-1 cell lines. (*D*) Seven-day lapatinib dose–response curves for HCC1954-Par (*Above*) and JIMT-1 (*Below*) vector controls and single STAT1 or STAT3 knockouts. (*E*) The same for double STAT1 + STAT3 knockouts. (*F*) Seven-day SNX631 dose–response curves for HCC1954-Par (*Above*) and JIMT-1 (below) vector controls, dKO STAT1/3, and dKO STAT3/1. (*G*) Seven-day dose–response curves for HCC1954-Par (*Above*) and JIMT-1 (*Below*) dKO STAT3/1 knockout to lapatinib, SNX631, and their combination.

Mice were randomized into four groups when the average tumor volume reached ∼100 to 150 mm^3 and treated with vehicle, SNX631, lapatinib, or SNX631 + lapatinib combination. Fig. 6*A* shows the effects of the treatments on tumor volumes (*Left*), final tumor weights (*Middle*), and mouse body weights (*Right*) for HCC1954-Par, and Fig. 6*B* shows the same data for HCC1954-Res xenografts. Lapatinib significantly inhibited tumor growth in both models, although its effect was stronger in HCC1954-Par than in HCC1954-Res tumors, as expected. Remarkably, SNX631 alone significantly decreased tumor size and tumor weights in both models, despite its weak effect in vitro against the same cells (Fig. 1 *A* and *B*), indicating in vivo–specific roles of CDK8/19 in $HER2^+$ tumors. The combination of lapatinib and SNX631 exhibited the strongest tumor growth inhibition in both models, significantly enhancing the effects of lapatinib and SNX631 (Fig. 6 *A* and *B*). There was no toxicity of the treatments based on mouse body weights and cage-side observations. (Fig. 6 *A* and *B*).

We carried out extensive immunohistochemical (IHC) and immunofluorescence (IF) analysis of HCC1954-Par tumors from all treatment arms; representative images are shown in *SI Appendix*, Figs. S4–S6. Hematoxylin and eosin (H&E) staining (*SI Appendix*, Fig. S4*A*) showed extensive tumor necrosis in all arms, including control, in agreement with previous characterization of this xenograft model (49). Both individual drugs and their combination strongly decreased staining for proliferation

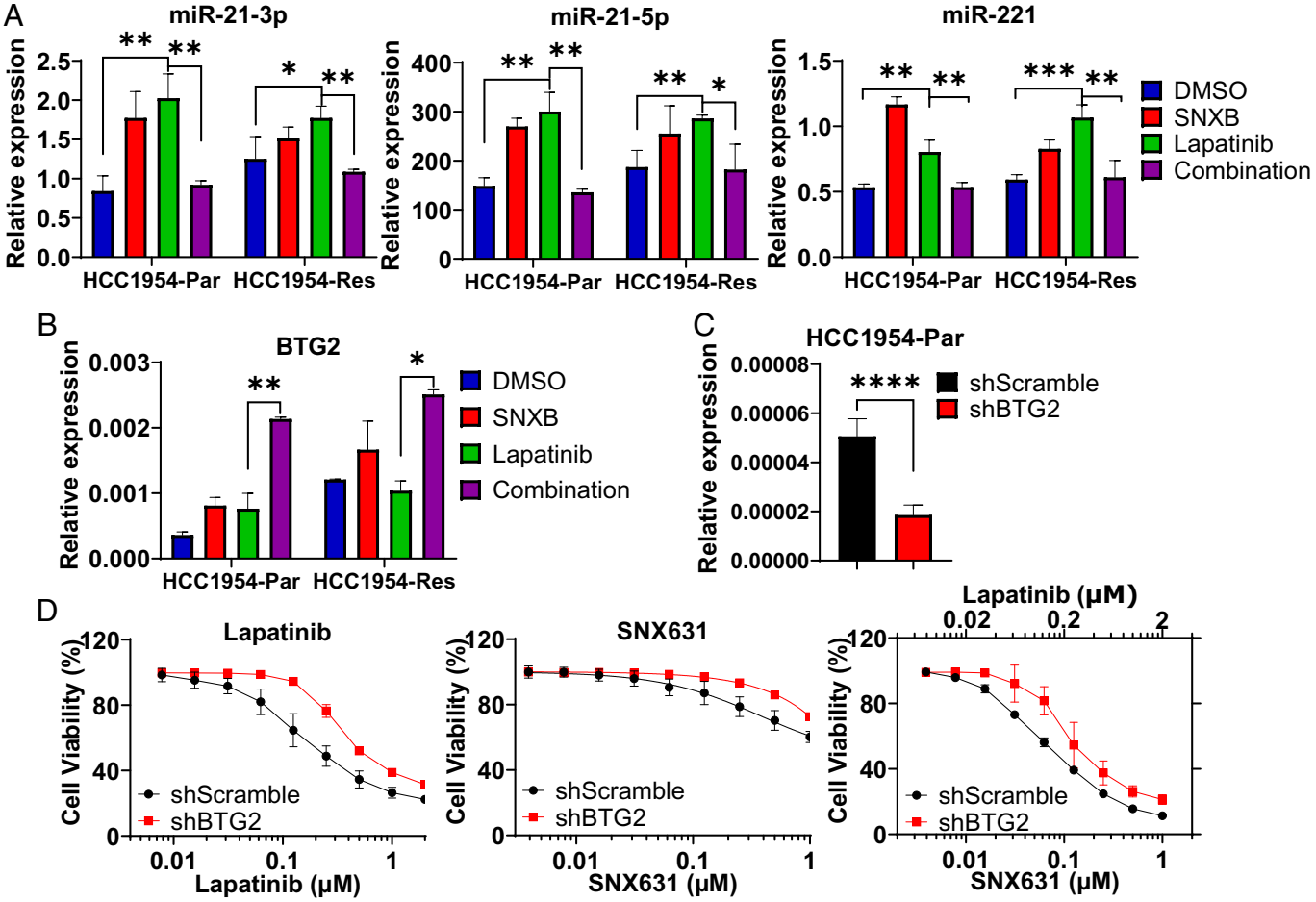

Fig. 5. Effects of lapatinib and CDK8/19i on miR-21, miR-221, and BTG2. (*A*) qPCR analysis of miR-21-3p, miR-21-5p, and mir-221 expression in HCC1954-Par and HCC1954-Res cells treated for 24 h with DMSO (control), senexin B, lapatinib, or senexin B + lapatinib combination. (*B*) The same analysis for BTG2 expression. (*C*) qPCR analysis of shRNA knockdown of BTG2 expression in HCC1954-Par cells. (*D*) Seven-day dose–response curves for the effects of lapatinib and SNX631, alone and in combination, and in HCC1954-Par cells transduced with BTG2 shRNA or scramble shRNA. *$P < 0.05$; **$P < 0.01$; ***$P < 0.001$; ****$P < 0.0001$.

marker Ki67 (Fig. 6*C* and *SI Appendix*, Fig. S4*B*). Apoptosis (as measured by Terminal deoxynucleotidyl transferase dUTP nick end labeling (TUNEL) staining), was increased by lapatinib and lapatinib + SNX631 but not by SNX631 alone (Fig. 6*D* and *SI Appendix*, Fig. S4*C*). HER2 expression was not detectably altered by any treatments (*SI Appendix*, Fig. S4*D*) and ERα expression remained almost undetectable in all arms (*SI Appendix*, Fig. S4*E*).

Further, we analyzed the expression of STAT1 and STAT3 phosphorylated at S727, as well as total STAT1 and STAT3 expression. Although lapatinib alone appeared to decrease both total STAT1 and pSTAT1-S727 immunolabeling, the ratio of pSTAT1-S727 to tSTAT1 was not significantly different between lapatinib and control arms. On the other hand, SNX631 alone and in combination with lapatinib significantly decreased the ratio of pSTAT1-S727 to tSTAT1 (Fig. 6*E* and *SI Appendix*, Fig. S5 *A* and *B*). Both drugs, individually and in combination, decreased immunolabeling for pSTAT3-S727 and (to a lesser extent) for total STAT3 (Fig. 6*F* and *SI Appendix*, Fig. S5 *C* and *D*). These results indicate that inhibition of pSTAT3-S727 and pSTAT1-S727 may be regarded as a potentially mechanistic pharmacodynamic marker of CDK8/19 inhibition in HER2$^+$ BrCa therapy.

Potentially significant effects of SNX631 + lapatinib combination were observed in the analysis of stromal elements of the tumors. In particular, lapatinib treatment significantly increased αSMA immunolabeling, a marker of tumor recruitment of stromal fibroblasts, but such an increase was not observed when lapatinib was combined with SNX631 (Fig. 6*G* and *SI Appendix*, Fig. S6*A*), suggesting that CDK8/19 inhibition may suppress this potentially tumor-promoting effect of lapatinib. Staining for arginase-1 (ARG1), a marker of alternatively activated (M2) macrophages that can promote tumor aggressiveness (50), was strongly decreased by SNX631 and lapatinib alone, with a slightly greater suppression of this tumor-promoting stromal component in combination-treated tumors (Fig. 6*H* and *SI Appendix*, Fig. S6*B*). The recruitment of endothelial cells (assessed by staining for CD31) was decreased by lapatinib and combination treatment but not by SNX631 alone (*SI Appendix*, Fig. S6*C*).

Discussion

We have found that CDK8 expression in HER2$^+$ BrCa is very strongly correlated with shorter RFS in treated patients, in agreement with earlier analysis of clinical correlations of CDK8 RNA (10, 20) or protein (21) expression with RFS in BrCa in general. Remarkably, the RFS correlation for CDK8 was stronger than for >99% of all genes, including all but one target of approved drugs. This correlation, however, was not observed in patients who remained untreated after sample collection, suggesting that the impact of CDK8 may be exerted primarily on

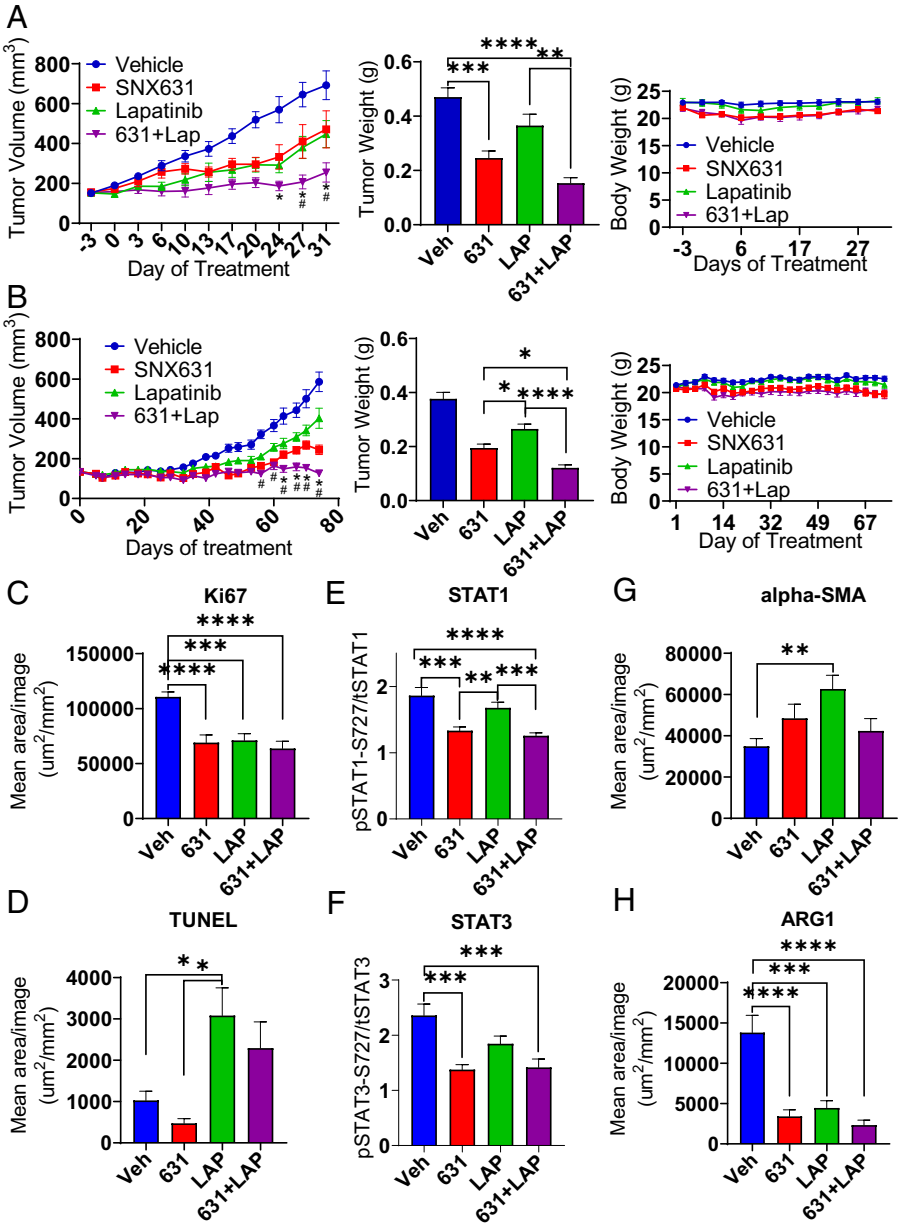

Fig. 6. Effects of SNX631 and lapatinib on HCC1954-Par and HCC1954-Res xenografts. (*A*) Tumor growth (*Top*), final tumor weights (*Middle*), and mouse body weights (*Bottom*) for HCC1954-Par xenografts treated with vehicle control, lapatinib, SNX631, and laptinib + SNX631 combination. (*B*) The same for HCC1954-Res xenografts. (*C*) Densitometric analysis of Ki67 IHC staining of HCC1954-Par xenografts treated with vehicle control, lapatinib, SNX631, and lapatinib + SNX631 combination (representative images in *SI Appendix*, Fig. S4*B*). (*D*) The same for TUNEL (apoptosis) staining (representative images in *SI Appendix*, Fig. S4*C*). (*E*) The same for IF staining for pSTAT1 S727 (representative images in *SI Appendix*, Fig. S5*A*), total STAT1 (representative images in *SI Appendix*, Fig. S5*B*), and ratio of IF image intensity for pSTAT1 S727 to total STAT1. (*F*) The same for pSTAT3 S727 and total STAT3 (representative images in *SI Appendix*, Fig. S5 *C* and *D*). For tumor growth: *SNX631 + lapatinib significantly different from SNX631 alone; #SNX631 + lapatinib significantly different from lapatinib alone. (*G*) The same for IF staining for αSMA (representative images in *SI Appendix*, Fig. S6*A*). (*H*) The same for IHC staining for arginase-1 (representative images in *SI Appendix*, Fig. S6*B*). For tumor mass and immunostaining: *$P < 0.05$; **$P < 0.01$; ***$P < 0.001$; ****$P < 0.0001$.

the response to treatment, which in the case of HER2$^+$ patients is centered on HER2-targeting drugs. This conclusion was validated by similar findings for other CDK module components, CCNC and MED13, although not for MED12, which previously showed dissimilar or even opposite prognostic correlations to other CDK module subunits (20). In agreement with the suggested impact of CDK8 on the outcome of treatment, two chemically distinct selective CDK8/19i strongly potentiated both trastuzumab and lapatinib (as well as neratinib) in all tested HER2$^+$ BrCa cell lines, including those that were resistant to trastuzumab or lapatinib alone, indicating that CDK8/19i may overcome resistance to HER2-targeting agents. CDK8/19 inhibition also prevented the development of lapatinib resistance in two HER2$^+$ BrCa cell lines, a result similar to the effects of these inhibitors we observed on the development of resistance to gefitinib and erlotinib (which target EGFR, a tyrosine kinase related to HER2/ERBB2) in HER2$^+$ BrCa cells (29). In the latter study, however, CDK8/19i did not potentiate the effects of EGFR inhibitors and did not overcome the acquired resistance to these agents, suggesting that the prevention of resistance was most likely due to the general ability of CDK8/19i to suppress transcriptional reprogramming (11). In contrast, the prevention of lapatinib resistance could have been due to the reversal of acquired resistance to lapatinib by CDK8/19 targeting drugs.

Since transcriptional regulation is the function of CDK8/19, we have used RNA-Seq to approach the mechanism of the

interaction between CDK8/19i and HER2 inhibitor lapatinib (which has a stronger and broader effect in vitro relative to the monoclonal antibody trastuzumab). Although lapatinib inhibits not only HER2 but also EGFR, the results of our analysis are unlikely to be attributable to EGFR inhibition, since CDK8/19 inhibition does not potentiate EGFR inhibitors in $HER2^+$ BrCa cells (29). GSEA analysis of the transcriptional effects of CDK8/19 and HER2 inhibitors suggested two pathways, PI3K/AKT/mTOR and IFNα/IFNγ, as potential mediators of synergy. Remarkably, even partial inhibition of PI3K by two chemically distinct inhibitors (pan-PI3K inhibitor pictilisib and PI3Kα-selective inhibitor alpelisib) strongly sensitized $HER2^+$ BrCa to lapatinib, in agreement with previous reports (51), and greatly diminished or abolished the synergy with CDK8/19i. This result suggests that inhibition of the transcriptional effects of the PI3K pathway by the combination of lapatinib and CDK8/19i could be largely responsible for the synergistic effect of the latter combination. On the other hand, given the effects of CDK8/19 on multiple transcription factors, it is unlikely to be the only mechanism.

In particular, CDK8/19 inhibition largely reversed the transcriptional effects of lapatinib on IFNα/IFNγ pathways, which are mediated in part by STAT transcription factors that are known to be phosphorylated at S727 residues by CDK8/19 (8, 13, 19, 35, 52, 53), although the effects of S727 phosphorylation on STAT-driven transcription are complex and cell context dependent (13, 35). STAT3 phosphorylation at S727 was reported to stimulate transcription of mitochondrial genes in zebrafish (54) but our RNA-Seq data showed no significant effects of treatments on any mitochondrial genes. STAT3, which as an established oncogenic driver in BrCa, was shown to be up-regulated (55) and potentiated (56) by HER2 and has been linked to resistance to HER2-targeting drugs in cell culture (57) and in the clinic (58). In contrast to STAT3, STAT1, which was also reported to be up-regulated by HER2 (59), is believed to play a tumor suppressor role in HER2-driven mammary tumor formation (38). Our analysis of the effects of STAT1 and STAT3 knockout showed drastic up-regulation of STAT1 upon STAT3 knockout in HCC1954 cells. This result, which suggests that STAT1 overexpression may compensate for the loss of STAT3 in $HER2^+$ BrCa growth, was surprising because STAT3 has been identified as a positive regulator of STAT1 expression (59). We have further found that the knockout of both STAT1 and STAT3, but not of the individual STATs, was required for sensitizing $HER2^+$ BrCa cells to lapatinib, also suggesting a compensatory mechanism.

We observed cooperative effects of HER2 and CDK8/19i on STAT1 and STAT3 phosphorylation at S727. We also noted a moderate decrease in the total STAT1 in cells treated with CDK8/19i. On the other hand, HCC1954 cells with the knockout of both STAT1 and STAT3 still showed a synergistic response to lapatinib and CDK8/19i, suggesting that the role of STATs in mediating this synergy may not be as prominent as the role of PI3K. As another potential mechanism, we found that oncogenic microRNAs miR-21 and miR-221, implicated in resistance to HER2-targeting drugs (42, 44), were up-regulated by lapatinib alone but not by lapatinib combination with a CDK8/19i, suggesting the prevention of lapatinib-induced induction of these miRNAs by CDK8/19i as a mechanism of synergy. In agreement with this hypothesis, we observed that stress-inducible tumor suppressor BTG2, a known target of miR-21, was up-regulated by a combination of lapatinib and a CDK8/19i in HCC1954 cells, and that BTG2 knockout increased cellular resistance to both lapatinib and the CDK8/19i. Taken together, our results indicate that CDK8/19 inhibition potentiates cell growth inhibition by HER2-targeting drugs through transcriptional effects on PI3K and other signal transduction pathways.

In vivo treatment of HCC1954-Par and HCC1954-Res xenografts with lapatinib, CDK8/19i SNX631, and their combination revealed that the addition of the CDK8/19i potentiated the effect of lapatinib and almost completely suppressed tumor growth in both models, with no apparent toxicity. Furthermore, SNX631 alone showed a significant tumor-suppressive effect, in contrast to its very weak effect on the proliferation of the same cells in vitro. Remarkably, CDK8/19i senexin B also showed an apparently more prominent effect on in vivo growth of ER^+ BrCa cells relative to its effect in vitro (10). Selective CDK8/19i have been shown to suppress the tumor-promoting paracrine activities of stromal fibroblasts (22), suggesting that the stronger in vivo effect of such inhibitors could be due to the role of CDK8/19 in tumor–stromal interactions. Indeed, we have observed that lapatinib-treated tumors had an increased content of tumor-associated αSMA-positive activated fibroblasts, but this increase was prevented by combining lapatinib with SNX631. Furthermore, SNX631 alone and in combination with lapatinib strongly decreased the content of ARG1-positive tumor-promoting M2 macrophages in tumor sections. Interestingly, M2 macrophage polarization is regulated by STATs, as are many other immune components of the tumor microenvironment (60). Our in vivo studies were based on xenograft models in immunodeficient mice, which lack the lymphocyte components. To overcome this limitation and to elucidate the impact of STAT-mediated and other effects of CDK8/19 on the immune components of the stroma, it will be necessary at the next phase to carry out in vivo studies using syngeneic tumor models in immunocompetent mice.

The results of the present study reveal that CDK8/19i partially suppress $HER2^+$ BrCa tumor growth and potentiate the effects of HER2-targeting drugs, the principal class of agents used in the treatment of such cancers. As previously reported, CDK8/19i also inhibit the growth of ER^+ BrCa and potentiate the effects of antiestrogens (10). Moreover, CDK8/19i were also found to inhibit the growth of triple negative BrCa (61, 62). These results suggest that CDK8/19i, some of which have already entered clinical trials, may become a key component in the therapeutic armamentarium for different types of BrCa.

Materials and Methods

The sources of all the materials, oligonucleotide sequences, and detailed methods are provided in *SI Appendix*.

Cell Modification and Cell Proliferation Assays. HCC1954 lapatinib-resistant cells were generated as described (27). sgRNA knockouts were carried out by lentiviral transduction of sgRNAs cloned in lentiCRISPR v2 vectors Addgene #52961 (from Feng Zheng) and Addgene #98293 (from Brett Stringer), followed by selection of transduced cells with puromycin or blasticidin, respectively. The effects of different compounds and their combinations on cell growth were measured by Sulphorhodamine B (SRB) assay after 7 d of treatment (or by acid phosphatase assay after 5 d of treatment in the case of neratinib). Synergy analysis was based on CI values calculated using CompuSyn software (28).

RNA and Protein Analysis. Expression of individual mRNAs or miRNAs in total RNA samples was measured by qRT-PCR. For miRNA analyses, total RNA was polyadenylated on the 3′ end prior to reverse transcription. RPL13A was used as the reference gene for qRT-PCR. RNA-Seq was carried out on Illumina HiSEq 3000/4000 platform for 2 × 150 bp reads, averaging ∼35 million reads per sample. DEG analysis was performed in R using the edgeR package. The GSEA analysis

was performed using Broad Institute GSEA software. The RNA-Seq data in Gene Expression Omnibus is available under accession No. GSE191050. For Western blot analysis, cell lysates were prepared using protease and phosphatase inhibitors. Protein bands were quantified with ImageJ.

Mouse Xenograft Models. Female NSG mice (aged 6 wk) were inoculated subcutaneously into the right flank with 5×10^6 HCC1954-Par or HCC1954-Res cells in 50% Matrigel. Tumors were measured with calipers and mice were weighed twice weekly. Once average tumor volume reached ~150 mm^3, mice were randomized to four treatment groups: control, SNX631 alone, lapatinib alone, or SNX631 + lapatinib. Lapatinib ditosylate was administered by daily oral gavage at 100 mg/kg. SNX631 was administered in a 500-ppm medicated diet (for the HCC1954-Par study) or in a 250-ppm medicated diet plus daily oral gavage supplement (5 mg/kg SNX631) (for the HCC1954-Res study). On the final day of the study, tumors were excised and weighed, and then fixed in 10% formalin and stored in 70% ethanol at 4 °C until processing. All mouse studies were approved by the University of South Carolina Institutional Animal Care and Use Committee.

IHC and IF Analysis. Immunostaining was carried out on 10-μm sections cut from formalin-fixed paraffin-embedded tissue blocks. For immunofluorescence, confocal imaging fields were selected that were within two field widths of the tumor boundary to avoid necrotic areas deeper in the tumor. A total of 4 to 10 fields per section were imaged. ImageJ scripts were used to convert original czi files into tiff images and create maximum intensity projections (MIPs). Image thresholds were set and verified using randomly selected subsets of MIPs.

Statistical Analysis. Differences between groups were validated by two-way/three-way analysis of variance (ANOVAs) with multiple comparisons, followed by *t* tests when validated, using GraphPad Prism 9 software. Kaplan–Meier survival analysis was carried out using www.kmplot.com on a total of 3,955 BrCas of Affymetrix microarray data, by selecting $HER2^+$ samples, further stratified as untreated or treated ("untreated excluded"). High expression of CDK8, CDK19 (CDC2L6), CCNC, MED12, and MED13 was defined as the upper tertile. The same analysis was repeated in all $HER2^+$ untreated excluded samples for all genes present in the gene arrays, using the JetSet best probeset. Druggable genes belonging to Tchem or Tclin categories (24) were identified using www.pharos.nih.gov.

Data Availability. RNA-Seq data have been deposited in Gene Expression Omnibus (GSE191050) and are available at (https://www.ncbi.nlm.nih.gov/geo/query/acc.cgi?acc=GSE191050) (63).

ACKNOWLEDGMENTS. We thank Taylor Dodd for her assistance with staining, imaging, and image analysis; and the Functional Genomics Core, the Drug Design and Synthesis Core, and the Microscopy and Flow Cytometry Core of the University of South Carolina Center for Targeted Therapeutics supported by grant P20 GM109091 for assistance with these studies. This research was funded by NIH grants P20 GM109091, R43CA213629 (E.V.B.), R44 CA203184 (M.C. and I.B.R.), American Cancer Society grant IRG-13-043-01 (E.V.B.), and Susan G. Komen postdoctoral fellowship PFD 15329865 (M.S.J.M).

Author affiliations: [a]Department of Drug Discovery and Biomedical Sciences, University of South Carolina College of Pharmacy, 715 Sumter St., Columbia, SC, 29208; [b]National Institute for Cellular Biotechnology, Dublin City University, Dublin 9, Ireland; [c]Department of Bioinformatics, Semmelweis University, Budapest, H-1085, Hungary; [d]Oncology Biomarker Research Group, Research Center for Natural Sciences, H-1117, Budapest, Hungary; and [e]Senex Biotechnology, Inc., 715 Sumter St., Columbia, SC, 29208

Author contributions: X.D., A.C.S., M.S.J.M., G.P.S., N.O., J.C., M.C., I.B.R., and E.V.B. designed research; X.D., A.C.S., M.S.J.M., G.P.S., A.C., H.J., J.L., L.Z., Z.T.M., L.I., N.O., B.G., M.C., I.B.R., and E.V.B. performed research; X.D., A.C.S., M.S.J.M., G.P.S., A.C., H.J., J.L., L.Z., Z.T.M., V.S., M.S., N.O., B.G., M.C., I.B.R., and E.V.B. analyzed data; and X.D., A.C.S., I.B.R., and E.V.B. wrote the paper.

1. G. Awada, A. Gombos, P. Aftimos, A. Awada, Emerging drugs targeting human epidermal growth factor receptor 2 (HER2) in the treatment of breast cancer. *Expert Opin. Emerg. Drugs* **21**, 91–101 (2016).
2. C. Vernieri *et al.*, Resistance mechanisms to anti-HER2 therapies in HER2-positive breast cancer: Current knowledge, new research directions and therapeutic perspectives. *Crit. Rev. Oncol. Hematol.* **139**, 53–66 (2019).
3. C. B. Fant, D. J. Taatjes, Regulatory functions of the Mediator kinases CDK8 and CDK19. *Transcription* **10**, 76–90 (2019).
4. R. Firestein *et al.*, CDK8 is a colorectal cancer oncogene that regulates beta-catenin activity. *Nature* **455**, 547–551 (2008).
5. C. Alarcón *et al.*, Nuclear CDKs drive Smad transcriptional activation and turnover in BMP and TGF-beta pathways. *Cell* **139**, 757–769 (2009).
6. A. Serrao *et al.*, Mediator kinase CDK8/CDK19 drives YAP1-dependent BMP4-induced EMT in cancer. *Oncogene* **37**, 4792–4808 (2018).
7. C. J. Fryer, J. B. White, K. A. Jones, Mastermind recruits CycC:CDK8 to phosphorylate the Notch ICD and coordinate activation with turnover. *Mol. Cell* **16**, 509–520 (2004).
8. J. Bancerek *et al.*, CDK8 kinase phosphorylates transcription factor STAT1 to selectively regulate the interferon response. *Immunity* **38**, 250–262 (2013).
9. M. D. Galbraith *et al.*, HIF1A employs CDK8-Mediator to stimulate RNAPII elongation in response to hypoxia. *Cell* **153**, 1327–1339 (2013).
10. M. S. McDermott *et al.*, Inhibition of CDK8 Mediator kinase suppresses estrogen dependent transcription and the growth of estrogen receptor positive breast cancer. *Oncotarget* **8**, 12558–12575 (2017).
11. M. Chen *et al.*, CDK8/19 Mediator kinases potentiate induction of transcription by NFκB. *Proc. Natl. Acad. Sci. U.S.A.* **114**, 10208–10213 (2017).
12. A. S. Adler *et al.*, CDK8 maintains tumor dedifferentiation and embryonic stem cell pluripotency. *Cancer Res.* **72**, 2129–2139 (2012).
13. I. Steinparzer *et al.*, Transcriptional responses to IFN-γ require Mediator kinase-dependent pause release and mechanistically distinct CDK8 and CDK19 functions. *Mol. Cell* **76**, 485–499.e8 (2019).
14. S. Osman *et al.*, The Cdk8 kinase module regulates interaction of the Mediator complex with RNA polymerase II. *J. Biol. Chem.* **296**, 100734 (2021).
15. T. Westerling, E. Kuuluvainen, T. P. Mäkelä, Cdk8 is essential for preimplantation mouse development. *Mol. Cell. Biol.* **27**, 6177–6182 (2007).
16. C. J. Lynch *et al.*, Global hyperactivation of enhancers stabilizes human and mouse naive pluripotency through inhibition of CDK8/19 Mediator kinases. *Nat. Cell Biol.* **22**, 1223–1238 (2020).
17. M. L. McCleland *et al.*, Cdk8 deletion in the Apc(Min) murine tumour model represses EZH2 activity and accelerates tumourigenesis. *J. Pathol.* **237**, 508–519 (2015).
18. P. A. Clarke *et al.*, Assessing the mechanism and therapeutic potential of modulators of the human Mediator complex-associated protein kinases. *eLife* **5**, e20722 (2016).
19. M. Chen *et al.*, Systemic toxicity reported for CDK8/19 inhibitors CCT251921 and MSC2530818 is not due to target inhibition. *Cells* **8**, 1413 (2019).
20. E. V. Broude *et al.*, Expression of CDK8 and CDK8-interacting genes as potential biomarkers in breast cancer. *Curr. Cancer Drug Targets* **15**, 739–749 (2015).
21. D. Xu *et al.*, Skp2-macroH2A1-CDK8 axis orchestrates G2/M transition and tumorigenesis. *Nat. Commun.* **6**, 6641 (2015).
22. D. C. Porter *et al.*, Cyclin-dependent kinase 8 mediates chemotherapy-induced tumor-promoting paracrine activities. *Proc. Natl. Acad. Sci. U.S.A.* **109**, 13799–13804 (2012).
23. B. Győrffy, Survival analysis across the entire transcriptome identifies biomarkers with the highest prognostic power in breast cancer. *Comput. Struct. Biotechnol. J.* **19**, 4101–4109 (2021).
24. T. Sheils *et al.*, How to illuminate the druggable genome using pharos. *Curr. Protoc. Bioinformatics* **69**, e92 (2020).
25. J. Li *et al.*, Characterizing CDK8/19 inhibitors through a NFκB-dependent cell-based assay. *Cells* **8**, 1208 (2019).
26. L. Zhang *et al.*, A selective and orally bioavailable quinoline-6-carbonitrile-based inhibitor of CDK8/19 mediator kinase with tumor-enriched pharmacokinetics. *J. Med. Chem.* **65**, 3420–3433 (2022).
27. M. S. McDermott *et al.*, PP2A inhibition overcomes acquired resistance to HER2 targeted therapy. *Mol. Cancer* **13**, 157 (2014).
28. T. C. Chou, Drug combination studies and their synergy quantification using the Chou-Talalay method. *Cancer Res.* **70**, 440–446 (2010).
29. A. C. Sharko *et al.*, The inhibition of CDK8/19 mediator kinases prevents the development of resistance to EGFR-targeting drugs. *Cells* **10**, 144 (2021).
30. R. Murad *et al.*, Transcriptome and chromatin landscape changes associated with trastuzumab resistance in HER2+ breast cancer cells. *Gene* **799**, 145808 (2021).
31. A. Subramanian *et al.*, Gene set enrichment analysis: A knowledge-based approach for interpreting genome-wide expression profiles. *Proc. Natl. Acad. Sci. U.S.A.* **102**, 15545–15550 (2005).
32. D. S. Green, H. A. Young, J. C. Valencia, Current prospects of type II interferon γ signaling and autoimmunity. *J. Biol. Chem.* **292**, 13925–13933 (2017).
33. M. H. Tsai, L. M. Pai, C. K. Lee, Fine-tuning of type I interferon response by STAT3. *Front. Immunol.* **10**, 1448 (2019).
34. A. Tesoriere, A. Dinarello, F. Argenton, The roles of post-translational modifications in STAT3 biological activities and functions. *Biomedicines* **9**, 956 (2021).
35. J. Martinez-Fabregas *et al.*, CDK8 fine-tunes IL-6 transcriptional activities by limiting STAT3 resident time at the gene loci. *Cell Rep.* **33**, 108545 (2020).
36. K. Banerjee, H. Resat, Constitutive activation of STAT3 in breast cancer cells: A review. *Int. J. Cancer* **138**, 2570–2578 (2016).
37. T. Mandal *et al.*, Reduced phosphorylation of Stat3 at Ser-727 mediated by casein kinase 2 - protein phosphatase 2A enhances Stat3 Tyr-705 induced tumorigenic potential of glioma cells. *Cell. Signal.* **26**, 1725–1734 (2014).
38. J. F. Raven *et al.*, Stat1 is a suppressor of ErbB2/Neu-mediated cellular transformation and mouse mammary gland tumor formation. *Cell Cycle* **10**, 794–804 (2011).
39. J. Liang *et al.*, CDK8 selectively promotes the growth of colon cancer metastases in the liver by regulating gene expression of TIMP3 and matrix metalloproteinases. *Cancer Res.* **78**, 6594–6606 (2018).
40. G. Kohanbash, H. Okada, MicroRNAs and STAT interplay. *Semin. Cancer Biol.* **22**, 70–75 (2012).
41. D. Bautista-Sánchez *et al.*, The promising role of miR-21 as a cancer biomarker and its importance in RNA-based therapeutics. *Mol. Ther. Nucleic Acids* **20**, 409–420 (2020).
42. B. Liu *et al.*, Serum microRNA-21 predicted treatment outcome and survival in HER2-positive breast cancer patients receiving neoadjuvant chemotherapy combined with trastuzumab. *Cancer Chemother. Pharmacol.* **84**, 1039–1049 (2019).
43. X. Yu *et al.*, Silencing of MicroRNA-21 confers the sensitivity to tamoxifen and fulvestrant by enhancing autophagic cell death through inhibition of the PI3K-AKT-mTOR pathway in breast cancer cells. *Biomed. Pharmacother.* **77**, 37–44 (2016).

44. T. K. Huynh *et al.*, miR-221 confers lapatinib resistance by negatively regulating $p27^{kip1}$ in HER2-positive breast cancer. *Cancer Sci.* **112**, 4234–4245 (2021).
45. J. Du *et al.*, MicroRNA-221 targets PTEN to reduce the sensitivity of cervical cancer cells to gefitinib through the PI3K/Akt signaling pathway. *Tumour Biol.* **37**, 3939–3947 (2016).
46. C. Zhang *et al.*, Global changes of mRNA expression reveals an increased activity of the interferon-induced signal transducer and activator of transcription (STAT) pathway by repression of miR-221/222 in glioblastoma U251 cells. *Int. J. Oncol.* **36**, 1503–1512 (2010).
47. S. Liu *et al.*, A microRNA 221- and 222-mediated feedback loop maintains constitutive activation of NFκB and STAT3 in colorectal cancer cells. *Gastroenterology* **147**, 847–859.e11 (2014).
48. B. Mao, Z. Zhang, G. Wang, BTG2: A rising star of tumor suppressors (review). *Int. J. Oncol.* **46**, 459–464 (2015).
49. B. Clinchy *et al.*, The growth and metastasis of human, HER-2/neu-overexpressing tumor cell lines in male SCID mice. *Breast Cancer Res. Treat.* **61**, 217–228 (2000).
50. S. Khabbazi, Y. Goumon, M. O. Parat, Morphine modulates interleukin-4- or breast cancer cell-induced pro-metastatic activation of macrophages. *Sci. Rep.* **5**, 11389 (2015).
51. E. Yao *et al.*, Suppression of HER2/HER3-mediated growth of breast cancer cells with combinations of GDC-0941 PI3K inhibitor, trastuzumab, and pertuzumab. *Clin. Cancer Res.* **15**, 4147–4156 (2009).
52. E. M. Putz *et al.*, CDK8-mediated STAT1-S727 phosphorylation restrains NK cell cytotoxicity and tumor surveillance. *Cell Rep.* **4**, 437–444 (2013).
53. Z. C. Poss *et al.*, Identification of mediator kinase substrates in human cells using cortistatin A and quantitative phosphoproteomics. *Cell Rep.* **15**, 436–450 (2016).
54. M. Peron *et al.*, Y705 and S727 are required for the mitochondrial import and transcriptional activities of STAT3, and for regulation of stem cell proliferation. *Development* **148**, ●●● (2021).
55. Z. Ren, T. S. Schaefer, ErbB-2 activates Stat3 alpha in a Src- and JAK2-dependent manner. *J. Biol. Chem.* **277**, 38486–38493 (2002).
56. W. Béguelin *et al.*, Progesterone receptor induces ErbB-2 nuclear translocation to promote breast cancer growth via a novel transcriptional effect: ErbB-2 function as a coactivator of Stat3. *Mol. Cell. Biol.* **30**, 5456–5472 (2010).
57. S. Aghazadeh, R. Yazdanparast, Activation of STAT3/HIF-1α/Hes-1 axis promotes trastuzumab resistance in HER2-overexpressing breast cancer cells via down-regulation of PTEN. *Biochim. Biophys. Acta, Gen. Subj.* **1861**, 1970–1980 (2017).
58. A. Sonnenblick *et al.*, Constitutive phosphorylated STAT3-associated gene signature is predictive for trastuzumab resistance in primary HER2-positive breast cancer. *BMC Med.* **13**, 177 (2015).
59. W. Han, R. L. Carpenter, X. Cao, H. W. Lo, STAT1 gene expression is enhanced by nuclear EGFR and HER2 via cooperation with STAT3. *Mol. Carcinog.* **52**, 959–969 (2013).
60. K. L. Polak, N. M. Chernosky, J. M. Smigiel, I. Tamagno, M. W. Jackson, Balancing STAT Activity as a Therapeutic Strategy. *Cancers (Basel)* **11**, 1716 (2019).
61. D. Kim *et al.*, Antitumor Activity of Vanicoside B Isolated from Persicaria dissitiflora by Targeting CDK8 in Triple-Negative Breast Cancer Cells. *J. Nat. Prod.* **82**, 3140–3149 (2019).
62. J. M. Spear, Z. Lu, W. A. Russu, Pharmacological Inhibition of CDK8 in Triple-Negative Breast Cancer Cell Line MDA-MB-468 Increases E2F1 Protein, Induces Phosphorylation of STAT3 and Apoptosis. Molecules 25 (2020).
63. X. Dinget *et al.*, Inhibition of CDK8/19 Mediator kinase potentiates HER2-targeting drugs and bypasses resistance to these agents in vitro and in vivo. Gene Expression Omnibus. https://www.ncbi.nlm.nih.gov/geo/query/acc.cgi?acc=GSE191050. Deposited 16 December 2021.